Quasi-Harmonic Lattice Dynamics of a Prototypical Metal–Organic Framework

Quasi-Harmonic Lattice Dynamics of a Prototypical Metal-Organic Framework

Matthew R. Ryder,[1,*] Jefferson Maul,[2] Bartolomeo Civalleri,[2] and Alessandro Erba[2,†]

[1] *Neutron Scattering Division, Oak Ridge National Laboratory, Oak Ridge, Tennessee 37831, United States of America*

[2] *Dipartimento di Chimica, Università di Torino, via Giuria 5, 10125, Torino, Italy*

(Dated: July 3, 2019)

Quasi-harmonic lattice-dynamical calculations are performed to investigate the combined effect of temperature and pressure on the structural and mechanical properties of a prototypical metal-organic framework material: MOF-5. The softening upon compression of an A_{2g} phonon mode at the Γ point in the high-symmetry F$m\bar{3}m$ structure is identified, which leads to a symmetry reduction and a group-subgroup phase transition to a low-symmetry F$m\bar{3}$ phase for compressions larger than 0.8%. The effect of the symmetry reduction on the equation-of-state of MOF-5 is investigated, which provides a static bulk modulus K reducing from 17 to 14 GPa and a corresponding change of K' (pressure derivative of K) from positive to negative. The effect of pressure on the negative thermal expansion of the framework and on its mechanical response is analyzed. The evolution of the mechanical anisotropy of MOF-5 as a function of pressure is also determined, which allows us to identify the occurrence of a shear-induced mechanical instability at 0.45 GPa.

I. INTRODUCTION

In the last two decades, quantum-mechanical simulations based on density functional theory (DFT) have arguably become the method of choice in the computational screening for advanced material design and crystal structure prediction of inorganic systems.[1] This is primarily due to a favorable balance between the accuracy and computational cost, and to the availability of several robust implementations in solid-state programs.[2–6] Owing to the efficient exploitation of high-performance computing (HPC) and to the development of a number of approaches to incorporate weak dispersive interactions in the exchange-correlation functional,[7–13] the last decade has also seen the successful application of DFT for computational screening of organic molecular crystals and metal-organic framework (MOF) materials.[14–19]

In this context, one of the main challenges DFT is currently facing is to reliably and efficiently describe the lattice dynamics of materials, as most of their energetic, structural, mechanical and functional properties are largely affected by thermal effects, even at room temperature.[20–22] Thermal effects are typically included within a statistical-thermodynamic approach by setting up a vibrational partition function in terms of harmonic lattice vibration frequencies. As an example, thermal effects have been included through the harmonic approximation (HA) to predict the most stable form of 508 polymorphic molecular crystals at room temperature; in 10% of the cases, a different polymorph was predicted with respect to static DFT calculations performed at 0 K.[23] By definition, the HA does not take into account the anharmonicity of the lattice dynamics,[24,25] which is known to affect several properties of materials significantly. Within the HA, thermal expansion is null, the elastic response of the system is independent of temperature, phonon lifetimes are infinite, lattice thermal conductivity is infinite, and constant-pressure and constant-volume thermodynamic properties coincide. Most of these limitations of the HA are due to approximating the volume to be constant and can be overcome using the so-called quasi-harmonic approximation (QHA), where the explicit dependence of the lattice vibrations on volume is taken into account.[26,27] The QHA not only describes the thermal expansion of the system and thus the thermal dependence of its elastic response, but also allows for combining temperature and pressure on the same thermodynamic footing.

While quasi-harmonic DFT calculations on the thermal properties of inorganic solids have been performed for the last 30 years,[28–38] the first applications of the methodology to organic molecular crystals were reported at the beginning of 2016.[39–41] In the last couple of years, dispersion-corrected DFT calculations with a quasi-harmonic treatment of lattice dynamical effects have then been successfully applied to study thermal properties of several molecular crystals,[42–46] which are often characterized by lower symmetry and larger numbers of atoms per unit cell with respect to simple inorganic systems. In this respect, MOFs are typically characterized by higher symmetry than molecular crystals but with a much larger number of atoms per unit cell. As a matter of fact, the possibility of successfully describing thermal features of MOFs by means of quasi-harmonic DFT lattice-dynamical calculations still represents an open challenge to state-of-the-art quantum-mechanical simulations. Indeed, after a pioneering quasi-harmonic study by Zhou *et al.* on the prototypical MOF-5 in 2008,[47] only very few studies have been reported on explicit quasi-harmonic DFT simulations on MOFs.[48–51]

It is well-known that MOF-5, as well as many other MOFs, exhibits negative thermal expansion (NTE), and the atomistic origin has been investigated both experimentally[52,53] and theoretically.[47,48,54,55] The NTE of MOF-5 is understood to arise from the presence of flexible carboxylate-based linkers bridging rigid ZnO_4 tetrahedra. However, little is known on the response of MOF-5 to pressure and in general on its mechanical proper-

ties.[56] Indeed, while the effect of pressure on the structure (pore size and negative thermal expansion) has been investigated by using penetrating pressure-transmitting media,[57,58] it has never been analyzed on the pristine framework (without adsorption of guest molecules in the pores). Therefore, the equation-of-state (EOS) and bulk modulus of pristine MOF-5 have never been quantified experimentally. Also, the directional elastic constants have never been measured experimentally. Instead, they have been computed with static DFT simulations at 0 K,[59] which provided values of $C_{11} = 21.5$ GPa, $C_{12} = 14.8$ GPa, and $C_{44} = 7.5$ GPa (with a corresponding static bulk modulus of $K = 17.0$ GPa). The value for the static bulk modulus of MOF-5 is in agreement with our present results, as we will discuss. On the contrary, the high reported value of 34 GPa for the bulk modulus of MOF-5 as well as its unphysical thermal dependence (with K increasing with temperature) make the quasi-harmonic methodology used by Wang *et al.* questionable.[48]

In this paper, we perform a quasi-harmonic lattice-dynamical investigation of the prototypical zinc-based MOF-5 and study the combined effect of temperature and pressure on its structure and mechanical response. First-principles DFT simulations are performed, where use is made of hybrid exchange-correlation functionals and where the effect of weak London-type dispersive interactions is explicitly investigated. Through the use of the Helmholtz free energies and the volumetric dependence of the phonon modes, we are able to compute the effect of temperature and pressure on the lattice dynamics and anisotropic mechanical properties. The results confirm the NTE of the crystalline lattice and additionally reveal a compression-induced phase transition, driven by the softening of a phonon mode at the Γ point, from the F$m\bar{3}m$ to the F$m\bar{3}$ space group.

II. COMPUTATIONAL DETAILS

All quantum-mechanical solid state calculations reported in this paper were performed with the CRYSTAL17 code.[6,60,61] The B3LYP hybrid exchange-correlation functional was used, augmented with a semi-empirical correction for dispersive interactions (B3LYP-D3), as suggested by Grimme and co-workers.[8] An all-electron basis set of triple-zeta quality was used for O, C and H,[62] as well as for Zn,[63] where the most diffuse s-type function was removed and a f-type polarization added. Reciprocal space was sampled in a Monkhorst-Pack net with a shrinking factor of 2, which corresponds to 3 points in the symmetry-irreducible Brillouin zone. All calculations (including geometry optimizations, vibration frequencies, and elastic constants) were performed with an energy threshold of 10^{-10} Ha for the self-consistent field (SCF) process.

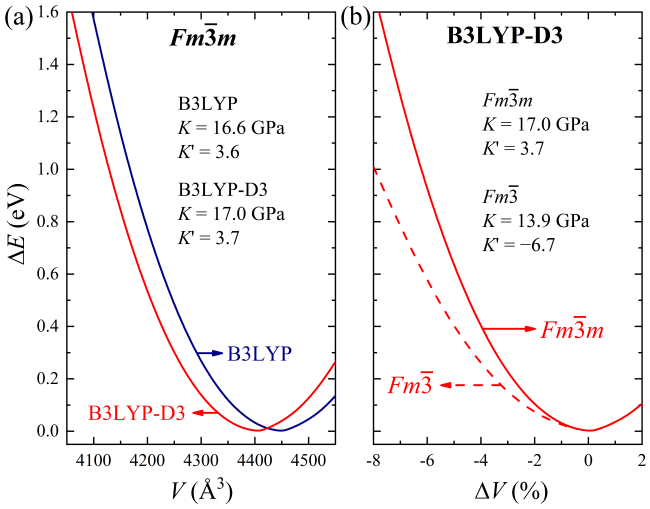

FIG. 1. Equation-of-state (EOS) of MOF-5. (a) the energy-volume EOS of the high-symmetry F$m\bar{3}m$ phase of MOF-5 as computed with (B3LYP-D3, red line) and without (B3LYP, blue line) the inclusion of dispersive interactions. (b) comparison between the energy-volume EOS of MOF-5 in its high-symmetry (F$m\bar{3}m$, continuous line) and low-symmetry phase (F$m\bar{3}$, dashed line).

III. RESULTS AND DISCUSSION

We started by investigating the static equation-of-state (EOS) of MOF-5 in its high-symmetry phase (F$m\bar{3}m$ space group) to discuss the structural and mechanical behavior upon compression and expansion. The atomic positions were fully relaxed at several volumes. The computed energy-volume curve is reported in Figure 1a and was fitted to the cubic Birch-Murnaghan EOS, which provided values for the bulk modulus $K = 16.6$ GPa and its pressure derivative $K' = \partial K/\partial P = 3.6$. A positive value of K' is found, which implies that the bulk modulus of the framework would increase with pressure for the high-symmetry phase. We also investigated the effect of taking into account weak dispersive interactions on the compressibility of the framework. The red line in Figure 1a is the energy-volume curve computed with the B3LYP-D3 method, compared to the blue line obtained with the B3LYP method. Overall, the inclusion of dispersive interactions results in a slight compression of the structure (by 0.4%) whereas all other features of the EOS are basically unchanged: the two curves are essentially parallel and are characterized by similar values of K and K'.

The lattice dynamics of the periodic framework and its localized vibrational modes were then calculated at a variety of specific volumetric compressions and expansions. Using the data obtained, we discovered the softening of the low-energy A_{2g} phonon mode on compression, which eventually becomes imaginary and leads to a structural (and mechanical) instability of the framework. By distorting the framework and reducing its symmetry accord-

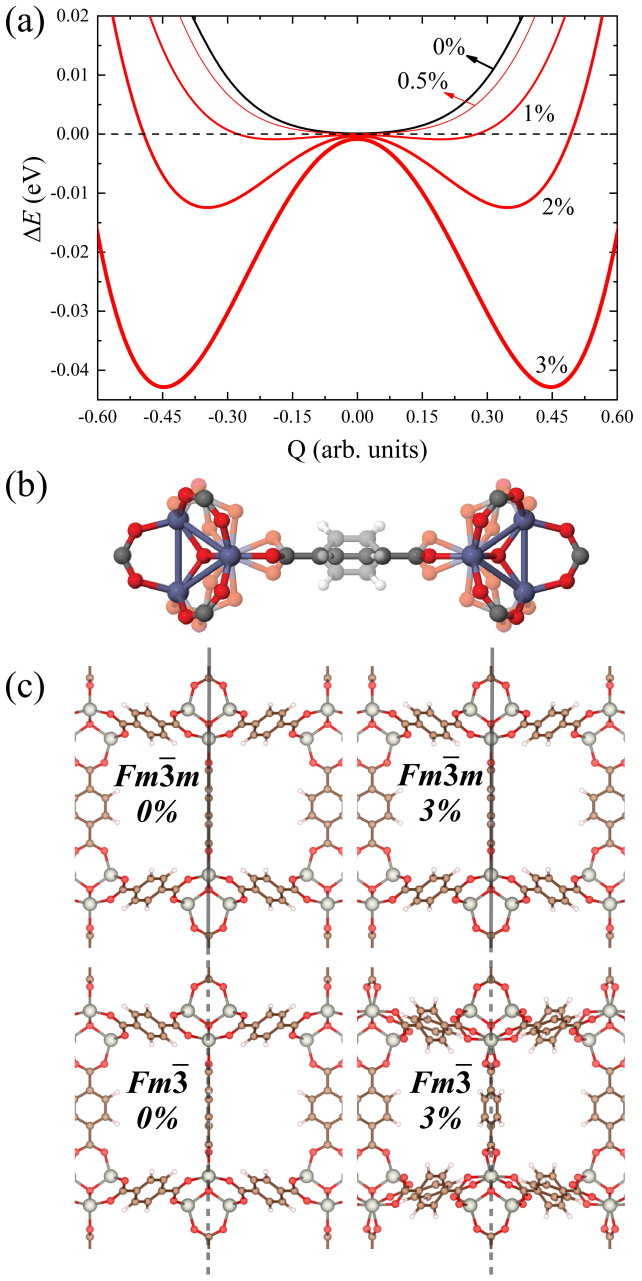

FIG. 2. Softening of the A_{2g} phonon mode using B3LYP in the high-symmetry F$m\bar{3}m$ structure leading to structural instability and a phase transition. (a) Energy profiles of MOF-5 as distorted along the A_{2g} normal coordinate Q at different levels of structural compression; (b) the nature of the A_{2g} normal mode and (c) the atomic structure of MOF-5 at the equilibrium volume and at a 3% compression in the high-symmetry and low-symmetry space groups.

ing to the A_{2g} normal mode, we could find a symmetry-reduced lattice configuration (space group F$m\bar{3}$) and resolve the structural instability on compression. This is shown in Figure 2 where the middle panel is a graphical representation of the A_{2g} normal mode, that can be described as a simultaneous deformation of the ZnO polyhedra (similar to that previously reported to be linked to the mechanical[64,65] and thermal[66] instability of other Zn-based MOF materials) and rotation of the organic linkers. This mode is also clearly linked to the mechanism underlying the NTE of the framework.[47,48,52–55] Figure 2a shows energy profiles of MOF-5 distorted along the A_{2g} normal coordinate Q at different levels of structural compression. The black line is the potential obtained by scanning the A_{2g} mode at the equilibrium volume, where the curvature is positive and corresponds to a positive harmonic frequency of 25 cm^{-1} (3.1 meV). At a compression of 0.5%, the computed harmonic frequency of the mode is still positive but has dropped to 8 cm^{-1} (1.0 meV). At further compressions (1%, 2% and 3% compressions are shown in the figure), the curvature becomes negative, the frequency imaginary, and two new symmetric minima are found along the A_{2g} normal coordinate, which correspond to a symmetry-broken nuclear configuration of F$m\bar{3}$ symmetry. The data reported in Figure 2 are obtained with the B3LYP method. The effect of dispersive interactions on the phonon softening was also studied by comparing the energetic differences when using the B3LYP and B3LYP-D3 functionals. The results confirmed the presence of a compression-induced phase transition and symmetry lowering both with and without the correction for dispersive interactions, the only difference being the occurrence of the imaginary frequency at slightly lower levels of compression for B3LYP-D3. Figure 2c shows the atomic structure of MOF-5 at the equilibrium volume and at a 3% compression in both the high-symmetry and low-symmetry space groups. It is seen that the lack of a mirror plane m in the F$m\bar{3}$ space group (dashed versus continuous grey vertical line) allows for the rotation of the linkers upon compression.

Let us stress that a very high numerical precision is needed in order to be able to perform such an analysis on a MOF and get such regular trends with compression. Indeed, the energy differences between the high-symmetry and low-symmetry phases while doing the scan of the A_{2g} mode are rather small, of the order of 0.01 eV, as documented in Figure 2. At this point, one might question the actual physical implications of such a symmetry breaking. However, Figure 1b shows that the equation-of-state of MOF-5 significantly changes on compression when the transition to the lower symmetry phase is allowed. In particular, the energy of MOF-5 lowers upon compression in the low-symmetry phase, which results in the change of the equilibrium bulk modulus from 17 to 14 GPa and, even more crucially, in the change of K' from positive to negative (3.7 in the high-symmetry structure and -6.7 in the low-symmetry structure). This latter change has important implications on the mechanical response of MOF-5 on pressure, which, if artificially constrained in the high-symmetry phase would stiffen upon compression, while, when given enough structural freedom, is found to soften upon compression.

Then, we studied the lattice dynamics of MOF-5

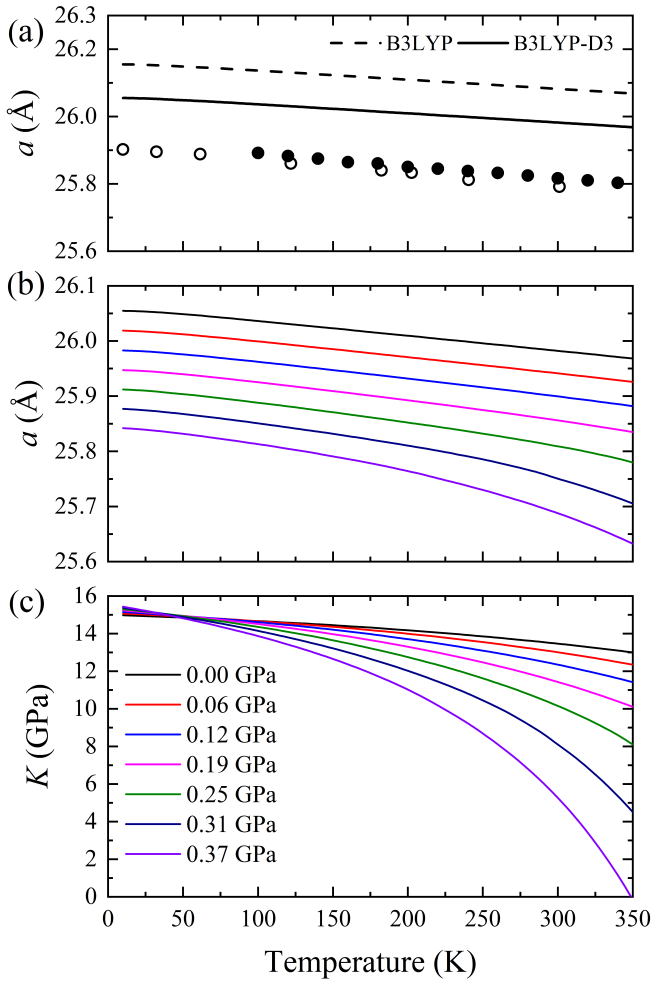

FIG. 3. Effect of temperature and pressure on the volume and bulk modulus of MOF-5 (in its low-symmetry F$m\bar{3}$ phase). (a) Thermal contraction of the lattice parameter of MOF-5 at zero pressure, as computed from quasi-harmonic lattice-dynamical calculations with B3LYP (dashed black line) and B3LYP-D3 (continuous black line), and as compared to experimental data from Ref. 47 (empty circles) and Ref. 52 (filled circles). (b) Lattice parameter of MOF-5 as a function of both temperature and pressure, as computed from quasi-harmonic B3LYP-D3 calculations. (c) Bulk modulus of MOF-5 as a function of both temperature and pressure, as computed from quasi-harmonic B3LYP-D3 calculations.

in the low-symmetry phase by using a quasi-harmonic methodology.[31,32] Phonon frequencies were computed at seven different volumes from a -5% compression to a 5% expansion (all computed frequencies were now positive in the whole explored volumetric range). The Helmholtz free energy $F(T,V)$ was computed, which, by minimization with respect to volume at different temperatures, leads to the determination of the thermal expansion of the system. The contraction of the lattice parameter with temperature is given in Figure 3a as computed with both the B3LYP and B3LYP-D3 methods, and compared to the experimental values reported in the literature showing NTE.[47,52] The agreement between the current theoretical results and the two experimental data sets in the literature is very satisfactory, both as regards the thermal dependence and the absolute value, particularly so with B3LYP-D3. In this respect, we collect in Table I all previous determinations of the linear thermal expansion coefficient of MOF-5 at room temperature: $\alpha_l = 1/a(\partial a/\partial T)$. Experimental values measured with powder X-ray diffraction and neutron diffraction span the range from -12 10^{-6} K^{-1} to -14.5 10^{-6} K^{-1}. Theoretical predictions from classical molecular dynamics (MD) to first-principles lattice-dynamical calculations span a larger range: from -8 10^{-6} K^{-1} to -18.3 10^{-6} K^{-1}, with our present result at -10.6 10^{-6} K^{-1}, which only slightly underestimates the experimental values.

Because of the NTE, both temperature and pressure produce a structural compression. The combined effect of temperature and pressure on the structure and average mechanical response (isothermal bulk modulus, $K = V(T)\partial^2 F(T,V)/\partial V^2$) of MOF-5 is reported in Figure 3b-c. The results show that the NTE is amplified with increasing pressure and that the bulk modulus of MOF-5 is characterized by a significant decrease as a function of combined thermal and mechanical stimuli.

To understand in more detail the extent of mechanical instability upon compression, we went beyond the analysis of the isotropic bulk modulus and investigated the effect of pressure on the anisotropic mechanical properties of MOF-5. We note that a full quasi-harmonic description of thermo-elasticity, as recently outlined in Ref. 68, is still rather challenging for MOFs. The single-crystal elastic constants of MOF-5 were computed, both with B3LYP and B3LYP-D3, at six different pressures (0.0, 0.1, 0.2, 0.3, 0.4 and 0.5 GPa),[69,70] which allowed us to determine the pressure dependence of a variety of mechanical properties. Figure 4a reports the bulk moduli of the F$m\bar{3}m$ and F$m\bar{3}$ phases, and shows the softening of the structure upon compression of the latter.

TABLE I. Coefficient of linear thermal expansion, α_l, at 300 K of MOF-5 as determined experimentally from powder X-ray diffraction (PXRD) and powder neutron diffraction (PND), and theoretically from molecular dynamics (MD) and lattice dynamics (LD) simulations.

Technique	α_l ($10^{-6}K^{-1}$)	Ref.
PXRD	-14.5	53
PXRD	-13.1	52
PND	-12.0	53
PND	-14.5	47
MD	-18.3	54
MD	-8.0	67
LD (QHA; PBE)	-17.6	47
LD (QHA; B3LYP-D3)	-10.6	This Study

The mechanical instability of MOF-5 upon compression is due to the softening of the shear elastic constant C_{44}, whose low value of about 1 GPa at the equilibrium volume almost linearly decreases with pressure so as to eventually fail the following Born condition for shear mechanical stability of cubic lattices under hydrostatic pressure:

$$C_{44} > P \tag{1}$$

Figure 4b shows the evolution with pressure of the quantity $(C_{44} - P)$, as computed with both the B3LYP and B3LYP-D3 methods. The inclusion of dispersive interactions produces slightly lower values for C_{44}. The stability condition is no longer satisfied for pressures above about 0.45 GPa, which corresponds to a compression of the structure of about 0.8%. We note that this type of shear mechanical instability is common to many zeolites and MOFs.[64,65,71–79] We followed the methodology outlined in Refs. 80 and 81 and recently applied to ZIF-8[75] to factorize the nuclear-relaxation contribution of the C_{44} elastic constant into contributions from specific phonon modes. In the low-frequency region of the vibrational spectrum, the largest contribution to the nuclear-relaxation softening of C_{44} is due to a phonon mode vibrating at 86 cm^{-1} (10.7 meV). The atomic motion of this phonon mode is reported in the inset of Figure 4b. Figure 4c shows the change in the directional shear moduli of MOF-5 with pressure, with the minimum shear modulus (in green) approaching zero above 0.45 GPa.

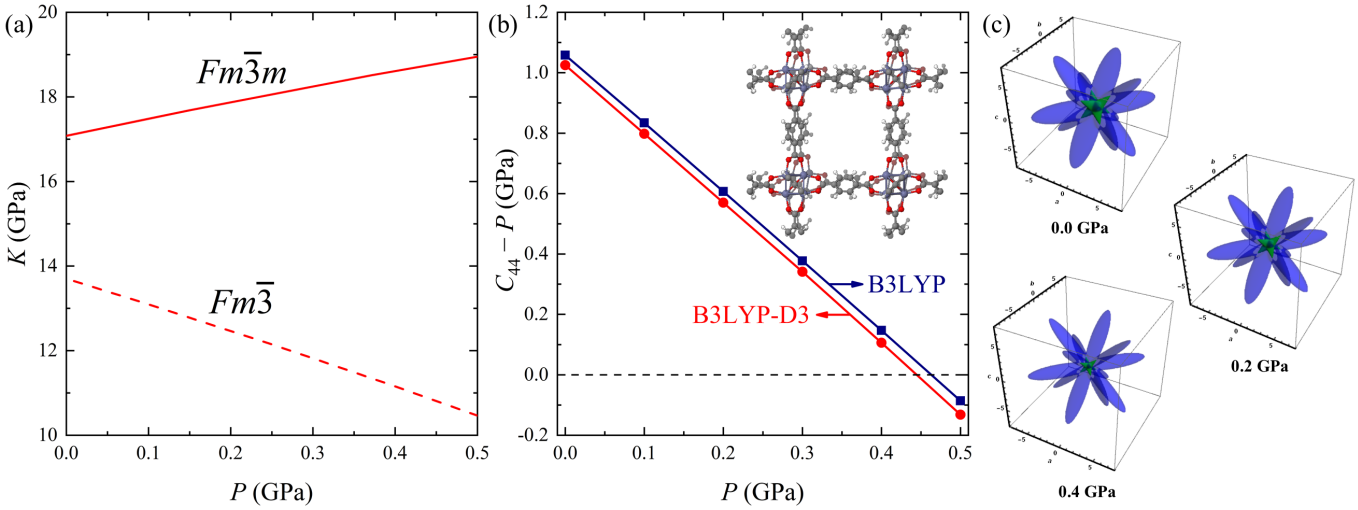

FIG. 4. Elastic moduli of MOF-5 as a function of pressure. (a) bulk modulus K as computed at B3LYP-D3 level for the high-symmetry (F$m\bar{3}m$, red continuous line) and low-symmetry (F$m\bar{3}$, red dashed line) structures. (b) shear instability of the F$m\bar{3}m$ phase with pressure (the inset is a graphical representation of the phonon mode that mostly contributes to the nuclear-relaxation of the shear C_{44} elastic constant). Values are computed with the B3LYP (blue lines) and B3LYP-D3 (red lines) methods. (c) 3D plots of the spatial distribution of the shear modulus from 0.0 to 0.4 GPa.

IV. CONCLUSIONS

In conclusion, we have shown that quasi-harmonic lattice-dynamics calculations are an effective method to study the combined effect of temperature and pressure on the structural and mechanical properties of porous framework materials. In addition, we show that the softening upon compression of low-energy phonon modes at the Γ point can revel symmetry-reducing group-subgroup phase transitions. For MOF-5, the transition is from F$m\bar{3}m$ to F$m\bar{3}$ for compressions larger than 0.8%. The results also highlight that a subtle structural transition can have a significant effect on the nature of the mechanical response, with the pressure derivative of the bulk modulus switching from positive to negative upon the reduction in symmetry.

ACKNOWLEDGEMENTS

M.R.R. acknowledges the U.S. Department of Energy Office of Science (Basic Energy Sciences) for research funding and the National Energy Research Scientific Computing Center (NERSC), a U.S. Department of Energy Office of Science User Facility operated under Contract No. DE-AC02-05CH11231 for access to supercom-

puting resources. M.R.R. would also like to thank Prof. Jin-Chong Tan for a discussion during the early stages of the work and the Engineering and Physical Sciences Research Council (EPSRC) for a Doctoral Prize Fellowship (EP/N509711/1) and the Rutherford Appleton Laboratory (RAL) for access to the SCARF cluster and additional computing resources. A.E. and J.M. thank the University of Torino and the Compagnia di San Paolo for funding (CSTO169372).

* rydermr@ornl.gov
† alessandro.erba@unito.it

[1] J. Hafner, C. Wolverton, and G. Ceder, *MRS Bulletin*, **2006**, *31*(9), 659–668.
[2] N. Varini, D. Ceresoli, L. Martin-Samos, I. Girotto, and C. Cavazzoni, *Comput. Phys. Commun.*, **2013**, *184(8)*, 1827 – 1833.
[3] F. Corsetti, *PLoS ONE*, **2014**, *9(4)*, e95390.
[4] J. Hutter, M. Iannuzzi, F. Schiffmann, and J. VandeVondele, *WIREs: Comput. Mol. Sci.*, **2014**, *4(1)*, 15–25.
[5] A. Maniopoulou, E. R. Davidson, R. Grau-Crespo, A. Walsh, I. J. Bush, C. R. A. Catlow, and S. M. Woodley, *Comput. Phys. Commun.*, **2012**, *183(8)*, 1696–1701.
[6] A. Erba, J. Baima, I. Bush, R. Orlando, and R. Dovesi, *J. Chem. Theory Comput.*, **2017**, *13*, 5019–5027.
[7] S. Grimme, J. Antony, S. Ehrlich, and H. Krieg, *J. Chem. Phys.*, **2010**, *132*, 154104.
[8] S. Grimme, J. Antony, S. Ehrlich, and H. Krieg, *J. Chem. Phys.*, **2010**, *132(15)*, 154104.
[9] J. Brandenburg and S. Grimme in *Prediction and Calculation of Crystal Structures*, ed. S. Atahan-Evrenk and A. Aspuru-Guzik, Vol. 345 of *Topics in Current Chemistry;* Springer International Publishing, **2014**; pp. 1–23.
[10] J. Moellmann and S. Grimme, *J. Phys. Chem. C*, **2014**, *118(14)*, 7615–7621.
[11] B. Civalleri, C. Zicovich-Wilson, L. Valenzano, and P. Ugliengo, *CrystEngComm*, **2008**, *10*, 405.
[12] A. Tkatchenko, R. A. DiStasio, R. Car, and M. Scheffler, *Phys. Rev. Lett.*, **2012**, *108*, 236402.
[13] A. M. Reilly and A. Tkatchenko, *J. Chem. Phys.*, **2013**, *139(2)*, 024705.
[14] M. A. Neumann and M.-A. Perrin, *J. Phys. Chem. B*, **2005**, *109(32)*, 15531–15541.
[15] C. Cazorla, *Coord. Chem. Rev.*, **2015**, *300*, 142 – 163.
[16] F.-X. Coudert and A. H. Fuchs, *Coord. Chem. Rev.*, **2016**, *307*, 211 – 236.
[17] S. L. Price, D. E. Braun, and S. M. Reutzel-Edens, *Chem. Commun.*, **2016**, *52*, 7065–7077.
[18] M. Witman, S. Ling, S. Anderson, L. Tong, K. C. Stylianou, B. Slater, B. Smit, and M. Haranczyk, *Chem. Sci.*, **2016**, *7*, 6263–6272.
[19] M. R. Ryder, L. Doná, J. G. Vitillo, and B. Civalleri, *ChemPlusChem*, **2018**, *83(4)*, 308–316.
[20] N. B. Bolotina, M. J. Hardie, R. L. Speer Jr, and A. A. Pinkerton, *J. Appl. Crystallogr.*, **2004**, *37(5)*, 808–814.
[21] T. B. Brill and K. J. James, *J. Phys. Chem.*, **1993**, *97(34)*, 8752–8758.
[22] A. O. Madsen, B. Civalleri, M. Ferrabone, F. Pascale, and A. Erba, *Acta Crystallogr. Sec. A*, **2013**, *69*, 309.
[23] J. Nyman and G. M. Day, *CrystEngComm*, **2015**, *17*, 5154–5165.
[24] A. Erba, J. Maul, M. Ferrabone, P. Carbonniére, M. Rérat, and R. Dovesi, *J. Chem. Theory Comput.*, **2019**, *15*, 3755–3765.
[25] A. Erba, J. Maul, M. Ferrabone, R. Dovesi, M. Rérat, and P. Carbonnière, *J. Chem. Theor. Comput.*, **2019**, *15*, 3766–3777.
[26] L. L. Boyer, *Phys. Rev. Lett.*, **1979**, *42*, 584.
[27] R. E. Allen and F. W. De Wette, *Phys. Rev.*, **1969**, *179*, 873–886.
[28] M. Catti, A. Pavese, and G. D. Price, *Phys. Chem. Minerals*, **1993**, *19(7)*, 472–479.
[29] K. Karch, P. Pavone, W. Windl, O. Schütt, and D. Strauch, *Phys. Rev. B*, **1994**, *50*, 17054–17063.
[30] S. Baroni, P. Giannozzi, and E. Isaev, *Reviews in Mineralogy and Geochemistry*, **2010**, *71(1)*, 39–57.
[31] A. Erba, *J. Chem. Phys.*, **2014**, *141*, 124115.
[32] A. Erba, M. Shahrokhi, R. Moradian, and R. Dovesi, *J. Chem. Phys.*, **2015**, *142*, 044114.
[33] A. Erba, J. Maul, R. Demichelis, and R. Dovesi, *Phys. Chem. Chem. Phys.*, **2015**, *17*, 11670–11677.
[34] A. Erba, J. Maul, M. De La Pierre, and R. Dovesi, *J. Chem. Phys.*, **2015**, *142*, 204502.
[35] J. Maul, I. M. G. Santos, J. R. Sambrano, and A. Erba, *Theor. Chem. Acc.*, **2016**, *135(2)*, 1–9.
[36] B. B. Karki and R. M. Wentzcovitch, *Phys. Rev. B*, **2003**, *68*, 224304.
[37] Z. Wu, R. M. Wentzcovitch, K. Umemoto, B. Li, K. Hirose, and J.-C. Zheng, *J. Geophys. Res.*, **2008**, *113*, B06204.
[38] J. M. Skelton, D. Tiana, S. C. Parker, A. Togo, I. Tanaka, and A. Walsh, *J. Chem. Phys.*, **2015**, *143(6)*, 064710.
[39] A. Erba, J. Maul, and B. Civalleri, *Chem. Commun.*, **2016**, *52*, 1820–1823.
[40] C. Cervinka, M. Fulem, R. P. Stoffel, and R. Dronskowski, *J. Phys. Chem. A*, **2016**, *120(12)*, 2022–2034.
[41] Y. N. Heit and G. J. O. Beran, *Acta Cryst. B*, **2016**, *72(4)*, 514–529.
[42] M. T. Ruggiero, J. Zeitler, and A. Erba, *Chem. Commun.*, **2017**, *53*, 3781–3784.
[43] J. G. Brandenburg, J. Potticary, H. A. Sparkes, S. L. Price, and S. R. Hall, *J. Phys. Chem. Lett.*, **2017**, *8*, 4319–4324.
[44] Y. N. Heit, K. D. Nanda, and G. J. O. Beran, *Chem. Sci.*, **2016**, *7*, 246–255.
[45] J. Hoja, A. M. Reilly, and A. Tkatchenko, *WIREs: Comput. Mol. Sci.*, **2017**, *7(1)*, e1294.
[46] S. R. Whittleton, A. Otero-de-la Roza, and E. R. Johnson, *J. Chem. Theory Comput.*, **2017**, *13(2)*, 441–450.
[47] W. Zhou, H. Wu, T. Yildirim, J. R. Simpson, and A. R. H. Walker, *Phys. Rev. B*, **2008**, *78*, 054114.
[48] L. Wang, C. Wang, Y. Sun, K. Shi, S. Deng, and H. Lu, *Mater. Chem. Phys.*, **2016**, *175*, 138 – 145.
[49] K. L. Svane, P. J. Saines, and A. Walsh, *J. Mater. Chem. C*, **2015**, *3*, 11076–11080.
[50] E. Cockayne, *J. Phys. Chem. C*, **2017**, *121(8)*, 4312–4317.
[51] A. E. Hoffman, J. Wieme, S. M. Rogge, L. Vanduyfhuys, and V. Van Speybroeck, *Zeitschrift für Kristallographie-Crystalline Materials*, **2019**.

[52] N. Lock, Y. Wu, M. Christensen, L. J. Cameron, V. K. Peterson, A. J. Bridgeman, C. J. Kepert, and B. B. Iversen, *J. Phys. Chem. C*, **2010**, *114(39)*, 16181–16186.

[53] N. Lock, M. Christensen, Y. Wu, V. K. Peterson, M. K. Thomsen, R. O. Piltz, A. J. Ramirez-Cuesta, G. J. McIntyre, K. Norén, R. Kutteh, C. J. Kepert, G. J. Kearley, and B. B. Iversen, *Dalton Trans.*, **2013**, *42*, 1996–2007.

[54] D. Dubbeldam, K. Walton, D. Ellis, and R. Snurr, *Angew. Chem. Int. Ed.*, **2007**, *46(24)*, 4496–4499.

[55] L. H. N. Rimmer, M. T. Dove, A. L. Goodwin, and D. C. Palmer, *Phys. Chem. Chem. Phys.*, **2014**, *16*, 21144–21152.

[56] J. D. Evans, and F. X. Coudert, *J. Am. Chem. Soc.*, **2016**, *138*, 6131–6134.

[57] N. Lock, M. Christensen, C. J. Kepert, and B. B. Iversen, *Chem. Commun.*, **2013**, *49*, 789–791.

[58] A. J. Graham, D. R. Allan, A. Muszkiewicz, C. A. Morrison, and S. A. Moggach, *Angew. Chem. Int. Ed.*, **2011**, *50(47)*, 11138–11141.

[59] M. Mattesini, J. M. Soler, and F. Ynduráin, *Phys. Rev. B*, **2006**, *73*, 094111.

[60] R. Dovesi, R. Orlando, A. Erba, C. M. Zicovich-Wilson, B. Civalleri, S. Casassa, L. Maschio, M. Ferrabone, M. De La Pierre, Ph. D'Arco, Y. Noël, M. Causá, M. Rérat, and B. Kirtman, *Int. J. Quantum Chem.*, **2014**, *114*, 1287–1317.

[61] R. Dovesi, A. Erba, R. Orlando, C. M. Zicovich-Wilson, B. Civalleri, L. Maschio, M. Rérat, S. Casassa, J. Baima, S. Salustro, and B. Kirtman, *WIREs Comput. Mol. Sci.*, **2018**, *8*, e1360.

[62] A. Schäfer, H. Horn, and R. Ahlrichs, *J. Chem. Phys.*, **1992**, *97(4)*, 2571–2577.

[63] A. Schäfer, C. Huber, and R. Ahlrichs, *J. Chem. Phys.*, **1994**, *100(8)*, 5829–5835.

[64] M. R. Ryder, B. Civalleri, T. D. Bennett, S. Henke, S. Rudić, G. Cinque, F. Fernandez-Alonso, and J.-C. Tan, *Phys. Rev. Lett.*, **2014**, *113*, 215502.

[65] M. R. Ryder and J.-C. Tan, *Dalton Trans.*, **2016**, *45*, 4154–4161.

[66] M. R. Ryder, T. D. Bennett, C. S. Kelley, M. D. Frogley, G. Cinque, and J.-C. Tan, *Chem. Commun.*, **2017**, *53*, 7041–7044.

[67] S. S. Han and W. A. Goddard, *J. Phys. Chem. C*, **2007**, *111(42)*, 15185–15191.

[68] M. Destefanis, C. Ravoux, A. Cossard, and A. Erba, *Minerals*, **2019**, *9*, 16.

[69] A. Erba, A. Mahmoud, R. Orlando, and R. Dovesi, *Phys. Chem. Miner.*, **2014**, *41*, 151–160.

[70] A. Erba, A. Mahmoud, D. Belmonte, and R. Dovesi, *J. Chem. Phys.*, **2014**, *140*, 124703.

[71] G. N. Greaves, F. Meneau, A. Sapelkin, L. M. Colyer, I. Gwynn, S. Wade, and G. Sankar, *Nat. Mater.*, **2003**, *2*, 622–629.

[72] N. Greaves and F. Meneau, *J. Phys.: Condens Matter*, **2004**, *16(33)*, S3459.

[73] G. N. Greaves, F. Meneau, O. Majérus, D. G. Jones, and J. Taylor, *Science*, **2005**, *308(5726)*, 1299–1302.

[74] W. Zhang, J. Maul, D. Vulpe, P. Z. Moghadam, D. Fairen-Jimenez, D. M. Mittleman, J. A. Zeitler, A. Erba, and M. T. Ruggiero, *J. Phys. Chem. C*, **2018**, *122(48)*, 27442–27450.

[75] J. Maul, M. R. Ryder, M. T. Ruggiero, and A. Erba, *Phys. Rev. B*, **2019**, *99*, 014102.

[76] A. U. Ortiz, A. Boutin, A. H. Fuchs, and F.-x. Coudert, *J. Phys. Chem. Lett.*, **2013**, *4(11)*, 1861–1865.

[77] M. R. Ryder, B. Civalleri, G. Cinque, and J.-C. Tan, *CrystEngComm*, **2016**, *18*, 4303–4312.

[78] M. R. Ryder, B. Civalleri, and J.-C. Tan, *Phys. Chem. Chem. Phys.*, **2016**, *18*, 9079–9087.

[79] M. R. Ryder, B. Van de Voorde, B. Civalleri, T. D. Bennett, S. Mukhopadhyay, G. Cinque, F. Fernandez-Alonso, D. De Vos, S. Rudić, and J.-C. Tan, Jun , **2017**, *118*, 255502.

[80] A. Erba, *Phys. Chem. Chem. Phys.*, **2016**, *18*, 13984–13992.

[81] A. Erba, D. Caglioti, C. M. Zicovich-Wilson, and R. Dovesi, *J. Comput. Chem.*, **2017**, *38*, 257–264.